

# Picosecond Phenomena III

Proceedings of the Third International Conference  
on Picosecond Phenomena  
Garmisch-Partenkirchen, Fed. Rep. of Germany  
June 16-18, 1982

Editors

K.B. Eisenthal   R.M. Hochstrasser   W. Kaiser  
A. Laubereau

With 288 Figures

Springer-Verlag Berlin Heidelberg New York 1982

# Contents

## *Part I*      **Advances in the Generation of Ultrashort Light Pulses**

Moving from the Picosecond to the Femtosecond Time Regime By C.V. Shank, R.L. Fork, and R.T. Yen .....	2
Femtosecond Optical Pulses: Towards Tunability at the Gigawatt Level By A. Migus, J.L. Martin, R. Astier, A. Antonetti, and A. Orszag ..	6
Femtosecond Continuum Generation. By R.L. Fork, C.V. Shank, R.T. Yen, C. Hirlimann, and W.J. Tomlinson .....	10
New Picosecond Sources and Techniques By A.E. Siegman and H. Vanherzeele .....	14
Generation of Coherent Tunable Picosecond Pulses in the XUV By T. Srinivasan, K. Boyer, H. Egger, T.S. Luk, D.F. Muller, H. Pummer, and C.K. Rhodes .....	19
New Infrared Dyes for Synchronously Pumped Picosecond Lasers By A. Seilmeier, B. Kopainsky, W. Kranitzky, W. Kaiser, and K.H. Drexhage .....	23
Acousto-Optic Stabilization of Mode-Locked Pulsed Nd:YAG Laser By H.P. Kortz .....	27
Active Mode Stabilization of Synchronously Pumped Dye Lasers By A.I. Ferguson and R.A. Taylor .....	31
Spectral Hole Burning in the Saturation Region of Mode-Locked Nd-Glass Lasers. By A. Penzkofer and N. Weinhardt .....	36
Single and Double Mode-Locked Ring Dye Lasers; Theory and Experiment By K.K. Li, G. Arjavalingam, A. Dienes, and J.R. Whinnery .....	40
Theoretical and Experimental Investigations of Colliding Pulse Mode-Locking (CPM). By W. Dietel, D. Kühlke, W. Rudolph, and B. Wilhelmi .....	45
Picosecond Carrier Dynamics and Laser Action in Optically Pumped Buried Heterostructure Lasers By T.L. Koch, L.C. Chiu, Ch. Harder, and A. Yariv .....	49
Optically Pumped Semiconductor Platelet Lasers in External Cavities By M.M. Salour .....	53

Two Photon Pumped Bulk Semiconductor Laser for the Generation of Picosecond Pulses. By Wei-Lou Cao, Fei-Ming Tong, De-Sen Shao, S.A. Strobel, V.K. Mathur, and Chi H. Lee .....	57
The Pulse Duration of a Distributed Feedback Dye Laser Under Single Pulse Conditions. By Z. Bor, B. Răcz, G. Szabó, and A. Müller .....	62
Picosecond Distributed Feedback Dye Laser Tunable in a Broad Spectral Range. By A.N. Rubinov, I. Chesnulyavichus, and T.Sh. Efendiev ....	66
Modelocking of a Wavelength Tunable High-Pressure CO <sub>2</sub> -Laser by Synchronous Modulation of a Broadband Intracavity Saturable Absorber. By J.K. Ajo, Y. Hefetz, and A.V. Nurmikko .....	68
The Non-Mode-Locked Picosecond Laser By F. Armani, F. DeMartini, and P. Mataloni .....	71
A Novel Method for Generating Sub-Transform Limited Picosecond Nd:YAG Laser Pulses. By S.C. Hsu and H.S. Kwok .....	74
Optical Dephasing in Inorganic Glasses By R.M. Shelby and R.M. MacFarlane .....	78
 <i>Part II     Ultrashort Measuring Techniques</i>	
Picosecond Holographic Grating Experiments in Molecular Condensed Phases. By M.D. Fayer .....	82
Self-Diffraction from Laser-Induced Orientational Gratings in Semiconductors. By A.L. Smirl, T.F. Boggess, B.S. Wherrett, G.P. Perryman, and A. Miller .....	87
A Picosecond Raman Technique with Resolution Four Times Better than Obtained by Spontaneous Raman Spectroscopy By W. Zinth, M.C. Nuss, and W. Kaiser .....	91
Broadband CARS Probe Using the Picosecond Continuum By L.S. Goldberg .....	94
Jitter-Free Streak Camera System By W. Knox, T.M. Nordlund, and G. Mourou .....	98
Electrical Transient Sampling System with Two Picosecond Resolution By J.A. Valdmanis, G. Mourou, and C.W. Gabel .....	101
High-Resolution Picosecond Modulation Spectroscopy of Near Interband Resonances in Semiconductors By S. Sugai, J.H. Harris, and A.V. Nurmikko .....	103
Electron Diffraction in the Picosecond Domain Steven Williamson and Gerhard Mourou and Synchronous Amplification of 70 fsec Pulses Using a Frequency-Doubled Nd:YAG Pumping Source. By J.D. Kafka, T. Sizer II, I.N. Duling, C.W. Gabel, and G. Mourou .....	107

Picosecond Time-Resolved Photoacoustic Spectroscopy By M. Bernstein, L.J. Rothberg, and K.S. Peters .....	112
Subpicosecond Pulse Shape Measurement and Modeling of Passively Mode- Locked Dye Lasers Including Saturation and Spatial Hole Burning By J.-C. Diels, I.C. McMichael, J.J. Fontaine, and C.Y. Wang .....	116
Experimental Demonstration of a New Technique to Measure Ultrashort Dephasing Times By J.C. Diels, W.C. Wang, P. Kumar, and R.K. Jain .....	120
Optical Pulse Compression with Reduced Wings By D. Grischkowsky and A.C. Balant .....	123
Polariton-Induced Compensation of Picosecond Pulse Broadening in Optical Fibers. By G.W. Fehrenbach and M.M. Salour .....	126
 <b>Part III Advances in Optoelectronics</b>	
Generation and Pulsewidth Measurement of Amplified Ultrashort Ultraviolet Laser Pulses in Krypton Fluoride. By P.H. Bucksbaum, J. Bokor, R.H. Storz, J.W. White, and D.H. Auston .....	130
Addressing and Control of High-Speed GaAs FET Logic Circuits with Picosecond Light Pulses By R.K. Jain, J.E. Brown, and D.E. Snyder .....	134
Surface Metal-Oxide-Silicon-Oxide-Metal Picosecond Photodetector By S. Thaniyavarn and T.K. Gustafson .....	137
Solid-State Detector for Single-Photon Measurements of Fluorescence Decays with 100 Picosecond FWHM Resolution By A. Andreoni, S. Cova, R. Cubeddu, and A. Longoni .....	141
Picosecond Optoelectric Modulation of Millimeter-Waves in GaAs Waveguide By M.G. Li, V.K. Mathur, Wei-Lou Cao, and Chi H. Lee .....	145
Synchroscan Streak Camera Measurements of Mode-Propagation in Optical Fibers. By J.P. Willson, W. Sibbett, and P.G. May .....	149
 <b>Part IV Relaxation Phenomena in Molecular Physics</b>	
Picosecond Lifetimes and Efficient Decay Channels of Vibrational Models of Polyatomic Molecules in Liquids By C. Kolmeder, W. Zinth, and W. Kaiser .....	154
Vibrational Population Decay and Dephasing of Small and Large Polyatomic Molecules in Liquids By H. Graener, D. Reiser, H.R. Telle, and A. Laubereau .....	159
Mechanisms for Ultrafast Vibrational Energy Relaxation of Polyatomic Molecules. By S.F. Fischer .....	164

Studies of the Generation and Energy Relaxation in Chemical Intermediates-Divalent Carbon Molecules and Singlet Oxygen By E.V. Sitzmann, C. Dupuy, Y. Wang, and K.B. Eisenthal .....	168
New Developments in Picosecond Time-Resolved Fluorescence Spectroscopy: Vibrational Relaxation Phenomena By B.P. Boczar and M.R. Topp .....	174
Picosecond Photon Echo and Coherent Raman Scattering Studies of Dephasing in Mixed Molecular Crystals By K. Duppen, D.P. Weitekamp, and D.A. Wiersma .....	179
Picosecond Laser Spectroscopy of Molecules in Supersonic Jets: Vibrational Energy Redistribution and Quantum Beats By A.H. Zewail .....	184
Picosecond Studies of Intramolecular Vibrational Redistribution in $S_1$ <i>p</i> -Difluorobenzene Vapor. By R.A. Coveleskie, D.A. Dolson, S.C. Muchak , C.S. Parmenter, and B.M. Stone .....	190
Direct Picosecond Resolving of Hot Luminescence Spectrum By J. Aaviksoo, A. Anijalg, A. Freiberg, M. Lepik, P. Saari, T. Tamm, and K. Timpmann .....	192
The Temperature Dependence of Homogeneous and Inhomogeneous Vibrational Linewidth Broadening Studies Using Coherent Picosecond Stokes Scattering. By S.M. George, A.L. Harris, M. Berg, and C.B. Harris	196
A Picosecond CARS-Spectrometer Using Two Synchronously Mode-Locked CW Dye Lasers. By J. Kuhl and D. von der Linde .....	201
Picosecond Studies of Intramolecular Charge Transfer Processes in Excited A-D Molecules By H. Staerk, R. Mitzkus, W. Kühnle, and A. Weller .....	205
Femtosecond Transient Birefringence in $CS_2$ By B.I. Greene and R.C. Farrow .....	209
Time-Resolved Observation of Molecular Dynamics in Liquids by Femtosecond Interferometry. By C.L. Tang and J.M. Halbout .....	212
Time-Resolved Measurement of Non-linear Susceptibilities by Optical Kerr Effect. By J. Etchepare, G. Grillon, R. Astier, J.L. Martin, C. Bruneau, and A. Antonetti .....	217
Subpicosecond Laser Spectroscopy: Pulse Diagnostics and Molecular Dynamics in Liquids. By C. Kalpouzos, G.A. Kenney-Wallace, P.M. Kroger, E. Quitevis, and S.C. Wallace .....	221
Viscosity-Dependent Internal Rotation in Polymethine Dyes Measured by Picosecond Fluorescence Spectroscopy By A.C. Winkworth, A.D. Osborne, and G. Porter .....	228
Rotational Diffusion in Mixed Solvents Measured by Picosecond Fluorescence Anisotropy. By T. Doust and G.S. Beddard .....	232

Investigation of Level Kinetics and Reorientation by Means of Double Pulse Excited Fluorescence By D. Schubert, J. Schwarz, H. Wabnitz, and B. Wilhelmi .....	235
Dynamics of Photoisomerization By G.R. Fleming, S.P. Velsko, and D.H. Waldeck .....	238
Evidence for the Existence of a Short-Lived Twisted Electronic State in Triphenylmethane Dyes By V. Sundström, T. Gillbro, and H. Bergström .....	242
Kinetics of Stimulated and Spontaneous Emission of Dye Solutions Under Picosecond Excitation. By B.A. Bushuk, A.N. Rubinov, A.A. Murav'ov, and A.P. Stupak .....	246
Picosecond Resolution Studies of Ground State Quantum Beats and Rapid Collisional Relaxation Processes in Sodium Vapor By R.K. Jain, H.W.K. Tom, and J.C. Diels .....	250
 <b>Part V Picosecond Chemical Processes</b>	
Unimolecular Processes and Vibrational Energy Randomization By R.A. Marcus .....	254
Picosecond Dynamics of I <sub>2</sub> Photodissociation. By P. Bado, P.H. Berens, J.P. Bergsma, S.B. Wilson, K.R. Wilson, and E.J. Heller .....	260
Vibrational Predissociation of S-Tetrazine-Ar van der Waals-Molecules By J.J.F. Ramaekers, J. Langelaar, and R.P.H. Rettschnick .....	264
Picosecond Laser Induced Fluorescence Probing of NO <sub>2</sub> Photofragments By P.E. Schoen, M.J. Marrone, and L.S. Goldberg .....	269
Excited State Proton Transfer in 2-(2-'Hydroxyphenyl)-Benzoxazole By G.J. Woolfe, M. Melzig, S. Schneider, and F. Dörr .....	273
Picosecond Dynamics of Unimolecular Ion Pair Formation By K.G. Spears, T.H. Gray, and D. Huang .....	278
Effect of Polymerization on the Fluorescence Lifetime of Eosin in Water By Wei-Zhu Lin, Yong-Lian Zhang, and Xin-Dong Fang .....	282
 <b>Part VI Ultrashort Processes in Biology</b>	
Picosecond Processes Involving CO, O <sub>2</sub> , and NO Derivatives of Hemeproteins. By P.A. Cornelius and R.M. Hochstrasser .....	288
Femtosecond and Picosecond Transient Processes After Photolysis of Liganded Hemeproteins. By J.L. Martin, C. Poyart, A. Migus, Y. Lecarpentier, R. Astier, and J.P. Chambaret .....	294
Picosecond Fluorescence Spectroscopy of Hematoporphyrin Derivative and Related Porphyrins By M. Yamashita, T. Sato, K. Aizawa, and H. Kato .....	298

Resonance Raman Spectra of Picosecond Transients: Application to Bacteriorhodopsin. By M.A. El-Sayed, Chung-Lu Hsieh, and M. Nicol	302
Picosecond Studies of Bacteriorhodopsin Intermediates from 11-cis Rhodopsin and 9-cis Rhodopsin. By J.-D. Spalink, M.L. Applebury, W. Sperling, A.H. Reynolds, and P.M. Rentzepis	307
Multiple Photon Processes in Molecules Induced by Picosecond UV Laser Pulses. By V.S. Antonov, E.V. Khoroshilova, N.P. Kuzmina, V.S. Letokhov, Yu.A. Matveetz, A.N. Shibanov, and S.E. Yegorov	310
P-BR and Its Role in the Photocycle of Bacteriorhodopsin By T. Gillbro and V. Sundström	315
Picosecond Linear Dichroism Spectroscopy of Retinal. By M.E. Lippitsch, M. Riegler, F.R. Aussenegg, L. Margulies, and Y. Mazur	319
Picosecond Absorption Spectroscopy of Biliverdin By M.E. Lippitsch, M. Riegler, A. Leitner, and F.R. Aussenegg	323
Picosecond Time-Resolved Resonance Raman Spectroscopy of the Photolysis Product of Oxy-Hemoglobin By J. Turner, T.G. Spiro, D.F. Voss, C. Paddock, and R.B. Miles	327
 <b>Part VII Applications in Solid-State Physics</b>	
Picosecond Time-Resolved Detection of Plasma Formation and Phase Transition in Silicon By J.M. Liu, H. Kurz, and N. Bloembergen	332
Spectroscopy of Picosecond Relaxation Processes in Semiconductors By D. von der Linde, N. Fabricius, J. Kuhl, and E. Rosengart	336
Picosecond Spectroscopy of Excitonic Molecules and High Density Electron-Hole Plasma in Direct-Gap Semiconductors. By S. Shionoya	341
Picosecond Time-Resolved Study of Highly Excited CuCl. By D. Hulin, A. Antonetti, L.L. Chase, G. Hamoniaux, A. Migus, and A. Mysyrowicz	345
Picosecond Dynamics of Excitonic Polariton in CuCl By Y. Aoyagi, Y. Segawa, and S. Namba	349
Picosecond Spectroscopy of Highly Excited GaAs and CdS By H. Saito, W. Graudszus, and E.O. Göbel	353
Non-Linear Attenuation of Excitonic Polariton Pulses in CdSe By P. Lavallard and P.H. Duong	357
Time-Resolved Photoluminescence Study of n Type CdS and CdSe Photoelectrode By D. Huppert, Z. Harzion, N. Croitoru, and S. Gottesfeld	360
Time-Resolved Spatial Expansion of the Electron-Hole Plasma in Polar Semiconductors By A. Cornet, T. Amand, M. Pagnet, and M. Brousseau	364

Weak-Wave Retardation and Phase-Conjugate Self-Defocusing in Si By E.W. Van Stryland, A.L. Smirl, T.F. Boggess, and F.A. Hopf .....	368
Ultrafast Relaxations of Photoinduced Carriers in Amorphous Semiconductors. By Z. Vardeny, J. Strait, and J. Tauc .....	372
Periodic Ripple Structures on Semiconductors Under Picosecond Pulse Illumination. By P.M. Fauchet, Zhou Guosheng, and A.E. Siegman ....	376
Transmission of Picosecond Laser-Excited Germanium at Various Wavelengths. By C.Y. Leung and T.W. Nee .....	380
Nonlinear Interactions in Indium Antimonide By M. Hasselbeck and H.S. Kwok .....	384
Picosecond Relaxation Kinetics of Highly Photogenerated Carriers in Semiconductors By S.S. Yao, M.R. Junnarkar, and R.R. Alfano .....	389
Picosecond Radiative and Nonradiative Recombination in Amorphous As <sub>2</sub> S <sub>3</sub> By T.E. Orłowski, B.A. Weinstein, W.H. Knox, T.M. Nordlung, and G. Mourou .....	395
<i>Index of Contributors</i> .....	399



# Picosecond Lifetimes and Efficient Decay Channels of Vibrational Models of Polyatomic Molecules in Liquids

C. Kolmeder, W. Zinth, and W. Kaiser

Physik Department der Technischen Universität München,  
D-8000 München, Fed. Rep. of Germany

Convincing evidence is presented that anharmonic coupling between fundamental vibrational modes and overtones or combination modes is of major importance for the lifetime of vibrational states. The selection rules known to hold for Fermi resonance determine the decay channels. In a number of examples the decay pathways of vibrational energy were observed experimentally by measuring the population and depopulation of subsequent vibrations. Drastic variations of vibrational lifetimes were found for different vibrations of the same molecule.

Molecules are first excited by an ultrashort resonant infrared pulse and the instantaneous degree of excitation is monitored by observing the anti-Stokes Raman signal of a delayed probe pulse. Different vibrational modes are distinguished by their characteristic anti-Stokes frequency.

We have investigated numerous molecules and found widely varying values of the population life-times between 1 ps and 240 ps in polyatomic molecules at room temperature /1,2/. Special attention was paid to the CH-stretching modes in the frequency range of  $3000 \pm 100 \text{ cm}^{-1}$ .

Vibrational energy is transferred from the CH-stretching modes ( $\sim 3000 \text{ cm}^{-1}$ ) via overtones and combination modes to lower energy states. Intramolecular anharmonic coupling, the Fermi resonance, manifests itself in the infrared and Raman spectra. Overtones and higher order combination modes borrow intensity from CH-stretching modes. We define as a measure of Fermi-resonance mixing the intensity ratio,  $R$ , between the final and initial state taken from the infrared or Raman spectrum. In a recent publication a formula was derived which allows to estimate the life time  $T_1$  of vibrational states:

$$T_1 = N(1-R)^2 R^{-1} \exp(\omega/\Omega)^{2/3} T_2(f) \quad (1)$$

$N$  corresponds to the number of states initially excited,  $R$  is a measure of the Fermi resonance, and  $T_2(f)$  stands for the dephasing time of the final state.  $T_2(f)$  may be estimated from the Raman line-width  $\Delta\tilde{\nu}$  as  $T_2(f) = (2\pi c \Delta\tilde{\nu})^{-1}$  ( $T_2(f)$  is equal to  $T_2/2$  measured in coherent Raman experiments). The frequency  $\omega$  represents the energy difference between the initial and final state.  $\Omega$  has a value close to  $100 \text{ cm}^{-1}$ .

As an example for the importance of Fermi resonance we present data of the two molecules 1,1-dichloroethene and trans 1,2-

dichloroethene which are made up of the same atoms; only two atoms have exchanged their positions. The infrared and Raman spectra between 2950  $\text{cm}^{-1}$  and 3250  $\text{cm}^{-1}$  of both molecules are depicted in Fig.1. There are drastic differences in the anharmonic coupling of the CH-stretching modes. In Fig.1a we see strong Fermi resonance of  $\text{CH}_2=\text{CCl}_2$  between the fundamental  $\nu_1$  and  $\nu_2+\nu_3$ , both of  $A_1$  symmetry and between the fundamental  $\nu_7$  and  $\nu_2+\nu_6+\nu_{11}$ , both of  $B_1$  symmetry /3/. This observation suggests that we have to consider at least two decay channels for the  $\text{CH}_2$ -stretching modes. For the decay  $\nu_1 \rightarrow \nu_2+\nu_3$  we estimate the intensity ratio  $R = 0.2 \pm 0.05$  and calculate  $T_2(f) = 0.3$  ps from the Raman line-width of  $\Delta\tilde{\nu} = 17$   $\text{cm}^{-1}$ . With  $N=1$  and  $\omega = 45$   $\text{cm}^{-1}$  we calculate from (1) a value of  $T_1 = 4 \pm 2$  ps. For the second decay channel  $\nu_7 \rightarrow \nu_2+\nu_6+\nu_{11}$  we have to take a short dephasing time  $T_2(f)$  of the combination mode. We estimate  $T_2(\nu_2+\nu_6+\nu_{11}) \approx 0.2$  ps from the observed line width. With  $R = 0.6 \pm 0.1$ ,  $N=1$  and  $\omega = 45$   $\text{cm}^{-1}$  we calculate  $T_1 = 1.5$  ps.

According to Figs.1a and 1b the symmetric ( $\nu_1$ ) and asymmetric ( $\nu_7$ )  $\text{CH}_2$ -stretching vibrations are separated by 100  $\text{cm}^{-1}$ . We estimate an energy-transfer time between the  $\text{CH}_2$ -stretching modes of  $T_1(\nu_1 \rightarrow \nu_7) \approx 3.3$  ps using the formula  $T_1(\omega_1 \rightarrow \omega_7) = T_2(\omega_1) \exp(\omega/\Omega)^{2/3}$ , where  $T_2(\omega_1)$  was taken from the Raman spectrum.

The estimates given here indicate that vibrational energy flows faster out of the  $\nu_7$  mode than it is supplied by the transfer  $\nu_1 \rightarrow \nu_7$ . For the excited and interrogated mode  $\nu_1$  we simply add the two decay rates for the two decay channels  $\nu_1 \rightarrow \nu_7$  and  $\nu_1 \rightarrow \nu_2+\nu_3$  and arrive at a lifetime  $T_1(\nu_1) \approx 2$  ps.

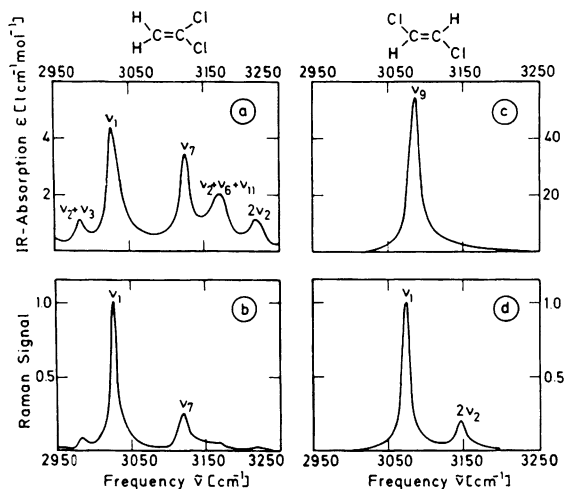


Fig.1 Infrared absorption (a) and Raman (b) spectra of  $\text{CH}_2\text{CCl}_2$  between 2950 and 3250  $\text{cm}^{-1}$ . Two combination tones are in strong Fermi resonance with the two CH-stretching modes  $\nu_1$  and  $\nu_7$ . Infrared absorption (c) and Raman (d) spectra of  $\text{trans-CHClCHCl}$ . There is less Fermi-resonance mixing than in  $\text{CH}_2\text{CCl}_2$ .

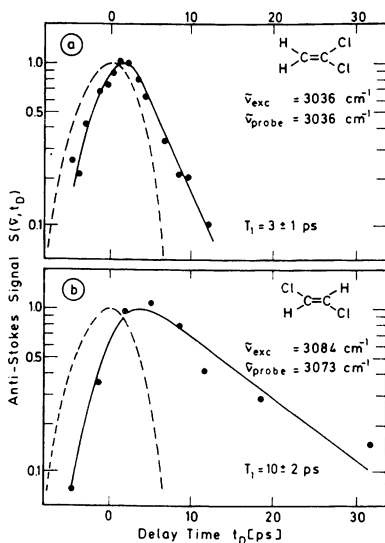


Fig.2 Anti-Stokes scattering signal versus delay time of the probing pulse. (a)  $\text{CH}_2\text{CCl}_2$  in  $\text{CCl}_4$  ( $c = 0.35$  m.f.). The decay of the  $\text{CH}_2$ -stretching mode at  $3036\text{ cm}^{-1}$  is shown. (b)  $\text{trans CHClCHCl}$  in  $\text{CCl}_4$  ( $c = 0.35$  m.f.). The  $\text{CH}$ -stretching mode at  $3084\text{ cm}^{-1}$  is excited and the mode at  $3073\text{ cm}^{-1}$  is monitored. The broken curves are the cross-correlation functions of the IR exciting and green probing pulses.

In Fig.2a we present experimental data of the direct determination of the  $T_1$  value. The scattered Raman signal of the  $\nu_1$  mode rises to a slightly delayed maximum during the excitation process and decays with a relaxation time of  $T_1$  discussed in the preceding paragraph. The broken curves in Fig.2 are cross-correlation curves of the excitation and probing pulse; they determine the zero point on the time axis and give a good indication of the time resolution of the experiment.

In Fig.1c we see the infrared active  $\text{CH}$ -stretching mode  $\nu_9$  and in Fig.1d the Raman active symmetric  $\nu_1$  mode of  $\text{trans CHClCHCl}$ . Here we find a considerably smaller Fermi resonance. The Raman spectrum of Fig.1d suggests some anharmonic coupling between  $\nu_1$  and  $2\nu_2$ , both of  $A_g$  symmetry  $/3/$ . With the values  $R = 0.15 \pm 0.02$ ,  $T_2 = 0.3\text{ ps}$ ,  $N=2$  and  $\omega = 80\text{ cm}^{-1}$  we calculate  $T_1 = 13\text{ ps}$ . It should be noted that there might be additional weak Fermi resonance between the  $\nu_9$  mode and higher combination modes (e.g.  $\nu_2 + \nu_5 + \nu_{10}$ ) buried under the high frequency tail of the  $\nu_9$  fundamental. These additional decay channels may reduce somewhat the estimated  $T_1$  value.

The time dependence of the  $\text{CH}$ -stretching modes of  $\text{trans CHClCHCl}$  is depicted in Fig.2b. The molecule is excited via the  $\nu_9$  mode at  $3084\text{ cm}^{-1}$  and the population of the  $\nu_1$  mode at  $3073\text{ cm}^{-1}$  is monitored by anti-Stokes Raman scattering. The rapid rise of the Raman signal, i.e. the fast population of the  $\nu_1$  mode, gives

clear evidence of the quick energy exchange between the two CH fundamentals  $\nu_1$  and  $\nu_9$ . The decay of the signal curve suggests a long lifetime of the two CH-stretching modes of  $T_1 = 10 \pm 2$  ps. This number is in good agreement with the value estimated above. The small intramolecular coupling gives rise to the longer vibrational life time.

The vibrational states of acetylene are well documented in the literature /4/. Inspection of the energy-level system (see Fig.3) suggests the following interesting situations:(i) Energy in the high lying CH-stretching modes around  $3200 \text{ cm}^{-1}$  readily flows into several combination modes, all of which comprise the symmetric C $\equiv$ C-stretching mode at  $\nu_2 = 1968 \text{ cm}^{-1}$ . (ii) The energy transfer from the  $\nu_2$  mode to neighboring combination modes is forbidden by symmetry selection rules. Thus we expect a long population life-time of the  $\nu_2$  mode.

Experimentally we investigated a solution of  $\text{C}_2\text{H}_2$  in  $\text{CCl}_4$ . Acetylene molecules first are vibrationally excited via the infrared active CH-stretching mode  $\nu_3 = 3287 \text{ cm}^{-1}$  and the population and depopulation of the  $\nu_2$  mode at  $1968 \text{ cm}^{-1}$  is monitored. In Fig.4 we indeed see a rapid population of the  $\nu_2$  mode within  $\leq 3$  ps and a very slow depopulation with a time constant of 240 ps. The  $\nu_2$  mode in acetylene represents a bottle-neck state. It exhibits the longest relaxation time observed so far in a polyatomic molecule in the liquid state at room temperature.

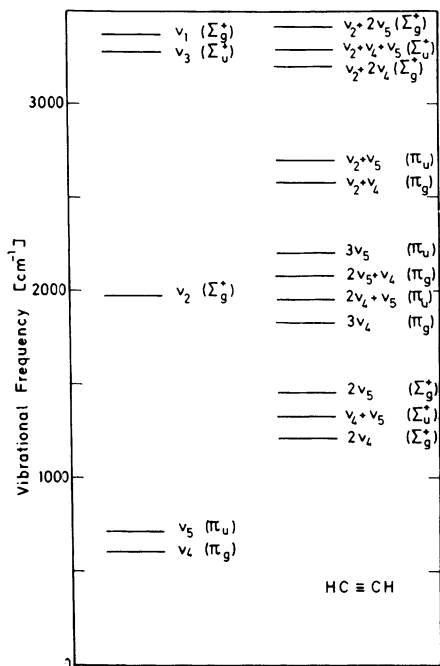


Fig.3 Energy-level diagram of Acetylene

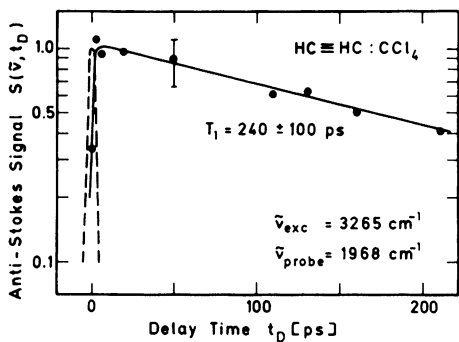


Fig. 4 Anti-Stokes scattering signal of  $C_2H_2$  in  $CCl_4$  versus delay time. Excitation frequency is  $3265\text{ cm}^{-1}$ . The decay of the  $C\equiv C$  mode at  $1968\text{ cm}^{-1}$  is monitored.

#### References

- 1 A. Fendt, S.F. Fischer, and W. Kaiser, *Chem. Phys.* 57, 55 (1981)
- 2 A. Fendt, S.F. Fischer, and W. Kaiser, *Chem. Phys. Lett.* 82, 350 (1981)
- 3 L.M. Sverdlov, M.A. Kovner, E.P. Krainov, *Vibrational Spectra of Polyatomic Molecules*, Wiley, New York, N.Y. 1974, and references therein
- 4 G. Herzberg, *Infrared and Raman spectra of Polyatomic Molecules* von Nostrand, Princeton, N.J. 1945